Soft Matter

COMMUNICATION

Cite this: *Soft Matter*, 2021, **17**, 810

Received 20th December 2020,
Accepted 11th January 2021

DOI: 10.1039/d0sm02240c

rsc.li/soft-matter-journal

Additive-induced ordered structures formed by $PC_{71}BM$ fullerene derivatives†

Pavel V. Komarov, *[ab] Maxim D. Malyshev,[a] Tsu-Che Yang,[c] Cheng-Ting Chiang,[c] Hu-Li Liao,[c] Daria V. Guseva,[b] Vladimir Yu. Rudyak,[d] Viktor A. Ivanov[de] and Shih-Huang Tung *[c]

We report the results of an experimental and theoretical study of structure formation in mixtures of phenyl-C_{71}-butyric acid methyl ester ($PC_{71}BM$) with high boiling octane based solvent additives 1,8-octanedithiol (ODT), 1,8-dibromooctane, and 1,8-diiodooctane obtained by evaporation of a host-solvent (chlorobenzene). Experimental studies by DSC, SAXS and WAXS methods found evidence of crystallization of fullerenes in the presence of the high boiling additives in the mixtures. A molecular dynamics simulation of a $PC_{71}BM$/ODT mixture revealed the self-assembly of fullerenes into sponge-like network structures.

Since their discovery, fullerenes have attracted the attention of a large number of researchers due to their unique electrochemical, photophysical, biological, and other properties.[1] Excellent electronic characteristics of these molecules (most of their derivatives belong to the class of small molecule n-type organic semiconductors) are important in creation of nonlinear optical materials and effective photovoltaic devices obtained by mixing with conductive polymers.[2] For (C_{60}-I_h)[5,6] fullerene (C60) and (C_{70}-$D_{5h(6)}$)[5,6]fullerene (C70), both nonpolar and low-polar aromatic compounds can be considered as "good" solvents. Despite the extremely high polarizability of the fullerene molecules, their solubility in polar solvents (acetone, acetonitrile, dimethyl sulfoxide, *etc.*) is negligible. Thus fullerenes should be modified for the preparation of various nanomaterials by solution processing technologies.[1,3] Surface modification of fullerenes with hydrophilic moieties gives them amphiphilic properties.[3] Depending on the chemical nature of the surface modifier, fullerene derivatives can self-assemble at the nanoscale into a wide variety of 1-D, 2-D and 3-D supramolecular architectures such as spheres, nanorods, nanotubules, fibers, disks, fractals, vesicles, *etc.*[3–5]

Soluble fullerene derivatives, such as [6,6]-phenyl-C_{61}-butyric acid methyl ester (PC61BM), [6,6]-phenyl-C_{71}-butyric acid methyl ester ($PC_{71}BM$), and indene-C_{60} bisadduct blended with conjugated polymers are used to form active layers of polymer solar cells (PSC).[6,7] Fullerenes and conjugated polymers mixed together in a so-called bulk heterojunction (BHJ) are not fully compatible in the solid phase, and their morphology, which develops during film formation, is kinetically arrested.[2,8] Many efforts have been made to retard their phase separation and thus to enhance the stability of devices. In particular, different functional groups were incorporated to enhance the miscibility between polymer matrices and fullerenes. It was noted that the use of combined solvents containing additives ("solvent additives"), such as octanethiol, diiodooctane and others, increases the power conversion efficiencies of PSC to 10% and higher.[9–12] Currently, the mechanism of solvent additives influence is not fully understood, however their use is a part of a universal strategy for producing highly effective PSCs. Two rules are used to select the host solvent and additives:[13] (i) the host solvent should dissolve all components of the mixture equally well, while additives should have selective solubility for one of the components (usually for acceptor), and (ii) additives should have higher boiling point than the host solvent. Following the above rules, many types of solvent additives were included in the processing of BHJ.[14,15] It was established that using additives facilitates integration of fullerene molecules into conjugated polymer matrices due to dissolution of their aggregates at late stage of film formation.[10,11,16]

Considering the ability of fullerenes to self-organize, it is important to study their behaviour in mixtures with host solvent and additives after evaporation of the host solvent. This should allow us to better understand the fundamental principles of the effect of high-boiling additives on the behaviour of fullerenes during the solution processing.

This paper presents the results of experimental study of the structure formation in mixtures of $PC_{71}BM$ (see Fig. 1a) with

[a] *Tver State University, Tver, 170100, Russia. E-mail: komarov.pv@tversu.ru*
[b] *A. N. Nesmeyanov Institute of Organoelement Compounds RAS, Moscow 119991, Russia*
[c] *Institute of Polymer Science and Engineering, National Taiwan University, Taipei 10617, Taiwan. E-mail: shtung@ntu.edu.tw*
[d] *Faculty of Physics, Lomonosov Moscow State University, 119991 Moscow, Russia*
[e] *Institut für Physik, Martin-Luther-Universität, Halle 06120, Germany*

† Electronic supplementary information (ESI) available. See DOI: 10.1039/d0sm02240c

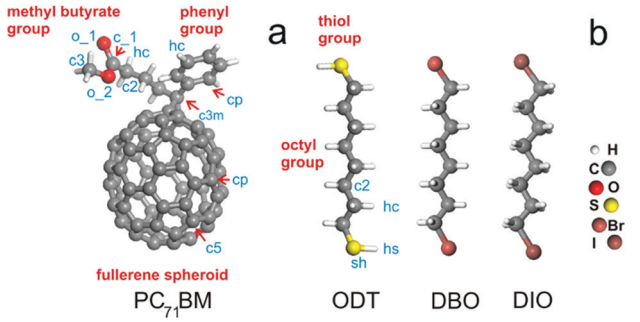

Fig. 1 Molecular structure of (a) the phenyl-C_{71}-butyric acid methyl ester; (b) high boiling point solvents, *viz.*, 1,8-octanedithiol (ODT), 1,8-dibromooctane (DBO), 1,8-diiodooctane (DIO). The figure contains definitions of types of atoms of the PCFF force field (small letters) and color representation of atoms (on the right).

octane based high boiling solvents 1,8-octanedithiol (ODT), 1,8-dibromooctane (DBO) and 1,8-diiodooctane (DIO) (see Fig. 1b) formed after evaporation of chlorobenzene which was used as a host solvent. To understand the obtained results, we investigated a structure of fullerenes aggregates formed due to their interaction with additives using full-atomistic molecular dynamics simulations of a model of the $PC_{71}BM$/ODT mixture.

Experimental methodology and results

We prepared the samples by dissolving $PC_{71}BM$ in chlorobenzene at ~25 mg/ml, and the high-boiling additives, including DIO, DBO, and ODT, were added into the solutions at desired amounts. The dissolution of active materials and additives in a common solvent is the general procedure to prepare devices, such as organic solar cells and transistors.[17,18] After completely mixing, chlorobenzene was removed in the vacuum oven for 1 h at room temperature. Due to the high boiling points of the additives, most of the additives remain in the samples after this process. Note that because $PC_{71}BM$ itself is soluble in DIO, DBO, and ODT, directly mixing $PC_{71}BM$ and the additives without the mediation of chlorobenzene can lead to the same results.

The small- and wide-angle X-ray scattering (SAXS and WAXS) data of pure $PC_{71}BM$ and the mixtures with the molar ratio of $PC_{71}BM$: additive = 1 : 8, which were obtained using beamline B23A1 in the National Synchrotron Radiation Research Centre (NSRRC), Taiwan,[19] are shown in Fig. 2. The original 2-D patterns are shown in Fig. S1 and S2 of ESI.† Note that the diffraction patterns of the samples at varying ratios (1 : 0.5–1 : 20) are similar, as shown in Fig. S3 (ESI†). After the removal of chlorobenzene, pure $PC_{71}BM$ (Fig. 2a) shows no characteristic diffraction in the SAXS profile, and only amorphous halos without distinct crystalline diffraction peaks are seen in the WAXS profile, indicating that pure $PC_{71}BM$ is in an amorphous state upon evaporation of chlorobenzene. In contrast, $PC_{71}BM$ mixed with the high boiling additives shows clear diffraction peaks both in the SAXS and WAXS profiles. The main peaks in the SAXS data for DIO, DBO, and ODT are at q = 0.25, 0.26, and 0.33 Å^{-1}, corresponding to d-spacing of

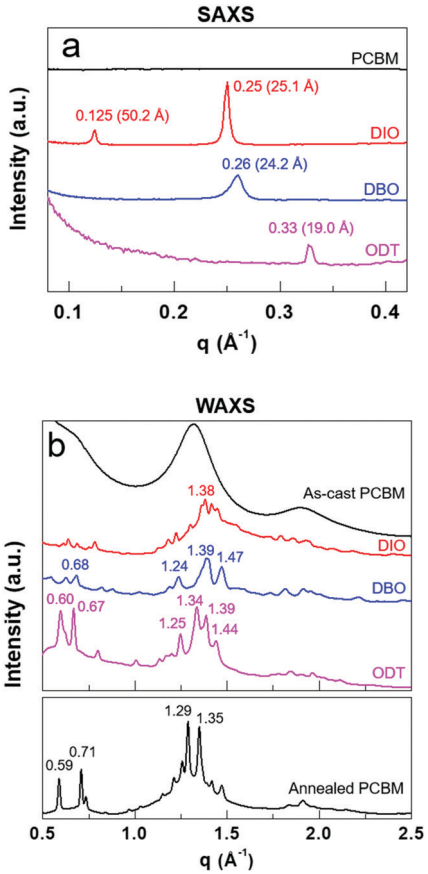

Fig. 2 (a) SAXS and (b) WAXS data of pure $PC_{71}BM$, mixtures with DIO, DBO, and ODT after casting from solutions, and pure $PC_{71}BM$ after annealing at 140 °C for 10 min.

25.1, 24.2, and 19.0 Å, respectively. This is an indication of ordered nanoscaled structures formed in the mixtures. An extra peak at q = 0.125 Å^{-1} (50.2 Å) for the DIO case implies that an even larger ordered structure is induced by DIO. Meanwhile, multiple sharp diffraction peaks appear in the WAXS profiles, manifesting a close packing of $PC_{71}BM$ molecules into crystalline aggregates in the presence of the liquid additives. Particularly, the crystalline structures induced by the additives are different from that of pure $PC_{71}BM$ thermally annealed at 140 °C (Fig. 2b), as evidenced by the different diffraction peaks. $PC_{71}BM$ and the additives may form co-crystals. An indication is that the 1.39 Å^{-1} peak (4.52 Å) only appears in the mixtures but is absent in pure $PC_{71}BM$. The size of the crystallites can be estimated by the Scherrer equation, $L = 5.56/\Delta q$, where Δq is the full width at half maximum (FWHM) of the diffraction peak.[20] The value Δq of the sharp peak at q = 0.67 Å^{-1} for the ODT case is ~ 0.02 Å^{-1}, which leads to a L ~ 278 Å. along the packing direction of the crystallographic planes that produce the peak. Combining the SAXS and WAXS data, we suggest that the additives induce a hierarchical structure with crystallites that stack regularly in a nanoscopic manner.

The data of the differential scanning calorimetry (DSC) measured at a heating rate of 10 °C min^{-1} for the as-cast samples are shown in Fig. 3. No phase transition occurs for

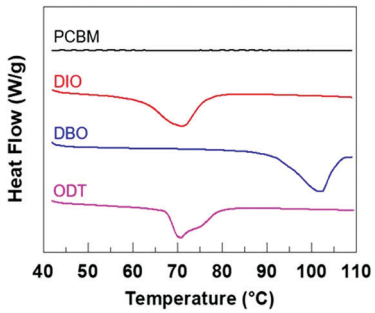

Fig. 3 DSC heating thermograms for pure $PC_{71}BM$ and its mixtures with DIO, DBO, and ODT after casting from solutions.

pure $PC_{71}BM$ below 110 °C, whereas endothermic transitions at 70.9, 102.2, and 70.6 °C are found for the DIO, DBO, and ODT cases, respectively. These transitions disappear in the second heating run after the samples are cooled down from 110 °C (the additives remain in the samples after this treatment), see Fig. S4 (ESI†), and simultaneously, the diffraction peaks originally shown in the SAXS profiles for the three additives disappear after heating to 110 °C (Fig. S5, ESI†). The endothermic peaks shown in the DSC data are thus the order–disorder transitions of the nanoscaled $PC_{71}BM$ structures revealed in the SAXS data, and the ordered structure is unable to rapidly form under cooling. Note that the structure can be restored in the cooled sample after annealing for 40 min at room temperature (Fig. S4, ESI†) and its SAXS diffraction pattern is the same as that before heating, indicating that it is a thermodynamically stable phase, not just a kinetically frozen one formed upon chlorobenzene evaporation.

Computer simulations

For computer simulations, we used the full-atomistic molecular dynamics (MD) method to clarify the nature of the structures formed by fullerenes in mixtures under the influence of high boiling additives. Since there is no suitable parameterization of the force field constants for compounds containing heavy halogen atoms (such as bromine and iodine) in currently used valence-force fields, we selected ODT as the solvent additive to investigate self-organization of the fullerene derivative $PC_{71}BM$.

All simulations were performed using the LAMMPS software package,[21,22] compiled with support for GPU accelerators and the class II polymer consistent force field (PCFF)[23] with additional parameters related to fullerene nanoparticle,[24] as was recommended in ref. 25–27 To construct the initial atomistic systems representing $PC_{71}BM$/ODT mixtures, we used the simulation protocol repeatedly used before.[28] Six statistically independent samples consisting of 32 $PC_{71}MB$, and 256 ODT molecules (the molar ratio 1 : 8) were constructed to eliminate the influence of the initial conditions on the structure formation. Fig. 1 provides information on atom types for the PCFF force field. More details on MD simulations are given in Section S2 in ESI.†

During the evolution of the constructed samples, a gradual formation of aggregates from fullerenes is observed. The structure of these aggregates stabilizes upon reaching 90 ns. This is

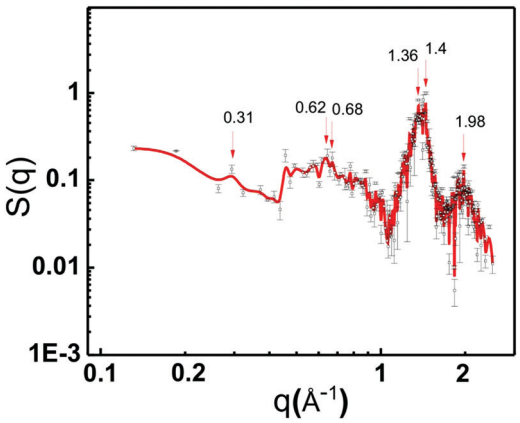

Fig. 4 The calculated static structure factor, $S(q)$, from our MD simulations of 200 ns duration. All atoms except hydrogens were taken into account. Its amplitude was normalized with respect to the values of the largest reflex $S(q^*)$.

confirmed by the partial structure factors $S(q)$ calculated for all atoms except hydrogens (see Fig. 4), and $S_{c5}(q)$ for all atoms c5 in five-membered rings of fullerene spheroid (see Fig. S6, ESI† and Fig. 1a), which indicate the appearance of stable characteristic scales in the system. Further simulations up to 208 ns have not shown significant changes in the structural ordering of the fullerenes, see Fig. S7 in ESI.†

A visualization of fullerene molecules inside the simulation cell in Fig. S8 (ESI†) demonstrates that the resulting structures have a similar mesh structure. This indicates the absence of the influence of the initial ordering and the simulation time on the result of the self-assembly of the fullerenes. The obtained morphology of the mixture can be characterized as a mesh structure (see Fig. 5) formed by two interpenetrating phases, namely, fullerenes and octane based additives.

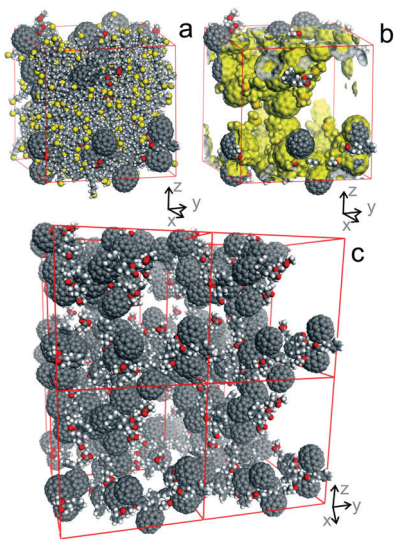

Fig. 5 Snapshot of the simulation box of $(5\ nm)^3$ after 200 ns: (a) the general view, (b) the $PC_{71}BM$ aggregate enclosed within the Connolly surface, (c) the simulation box is replicated 2 times along the x, y, z-directions to better visualize the periodic nature of the arisen aggregate. Coloring of atoms is the same as in Fig. 1. The additive molecules are not shown in (b) and (c) planes.

The position of the maxima on $S(q)$ obtained during the MD simulation in the wide-angle region q = 0.5–2.5 Å^{-1} (see Fig. 4) is consistent with the range of multiple diffraction peaks in WAXS data (see Fig. 2b). In addition, Fig. 4 shows a maximum in the small-angle region $q \sim 0.31$ Å^{-1}, corresponding to the distances of ~20.3 Å, which is close to the distinct peak at ~ 0.33 Å^{-1} (19.0 Å) for the ODT case shown in Fig. 2a. This points out the existence of a characteristic length scale for structural heterogeneities in the distribution of the fullerenes and the ODT molecules in the simulation cell volume.

The reasonable agreement between the obtained experimental data and simulation results indicates that the atomistic model of the ODT/$PC_{71}BM$ mixture captures the peculiarities of the structural organization of the real system rather well. More details about the local ordering in the system under study are given in Section S5 in ESI.†

Conclusions

In this communication, we report the first (to the best of our knowledge) observation of molecular self-assemblies of the phenyl-C_{71}-butyric acid methyl ester in mixtures with the high boiling octane based additives such as ODT, DBO and DIO, resulting from the evaporation of the host solvent. The studies by X-ray diffraction and calorimetry methods reveal the formation of the periodic structures with characteristic scales of similar length for all additives used and their destruction at high temperatures. These structures are presumably crystalline aggregates with hierarchical scales inside (from 4–5 Å for distances between fullerene molecules and about 20 Å for mesh size of network of their filament-like aggregates up to about 280 Å for size of such crystallites).

To interpret the experimental data, we performed the molecular dynamics simulation of the $PC_{71}BM$/ODT mixture at the fixed mass fraction of the ODT solvent and observed the aggregation of $PC_{71}BM$ molecules in a topologically complex sponge-like network. The hydrophobic part and the hydrophilic head group make it possible for $PC_{71}BM$ to assemble into 3D structures in the high boiling additives. In our opinion, this is possible due to the delicate balance between interactions of the fullerene spheroids, the surface modifier, and the additive molecules. To clarify the details of the self-assembly mechanism of $PC_{71}BM$ in the mixture with ODT molecules, we plan to carry out additional large-scale MD simulations.

Thus, the high boiling octane based additives can facilitate $PC_{71}BM$ to form 3D periodic aggregates. We believe that the results are useful for a better fundamental understanding of the effect of additives on the evolution of conjugated polymer/fullerene derivatives mixtures that is the key factor for the design of the new high effective organic photovoltaic devices.

Conflicts of interest

There are no conflicts to declare.

Acknowledgements

The financial support of the Russian Foundation for Basic Research (project 19-53-52004), the Ministry of Science and Technology of Taiwan (Project MOST 108-2923-E-002-001-MY3), and the Ministry of Science and Higher Education of the Russian Federation are highly appreciated. The X-ray scattering experiments were conducted in the National Synchrotron Radiation Research Center, Taiwan. The simulation was carried out using the equipment of the shared research facilities of HPC computing resources at Lomonosov Moscow State University.[29]

References

1 M. Prato and M. Maggini, *Acc. Chem. Res.*, 1998, **31**, 519–526.
2 L. Lu, T. Zheng, Q. Wu, A. M. Schneider, D. Zhao and L. Yu, *Chem. Rev.*, 2015, **115**, 12666–12731.
3 N. O. M. Hedlov-Petrossyan, *Chem. Rev.*, 2013, **113**, 5149–5193.
4 N. Nakashima, T. Ishii, M. Shirakusa, T. Nakanishi, H. Murakami and T. Sagara, *Chemistry*, 2001, **7**, 1766–1772.
5 V. Georgakilas, F. Pellarini, M. Prato, D. M. Guldi, M. Melle-Franco and F. Zerbetto, *Proc. Natl. Acad. Sci. U. S. A.*, 2002, **99**, 5075–5080.
6 G. Yu, J. Gao, J. C. Hummelen, F. Wudl and A. J. Heeger, *Science*, 1995, **270**, 1789–1791.
7 B. C. Thompson and J. M. J. Fréchet, *Angew. Chem., Int. Ed.*, 2007, **47**, 58–77.
8 B. A. Collins, E. Gann, L. Guignard, X. He, C. R. McNeill and H. Ade, *J. Phys. Chem. Lett.*, 2010, **1**, 3160–3166.
9 Y. Liang, Z. Xu, J. Xia, S.-T. Tsai, Y. Wu, G. Li, C. Ray and L. Yu, *Adv. Mater.*, 2010, **22**, E135–8.
10 S. J. Lou, J. M. Szarko, T. Xu, L. Yu, T. J. Marks and L. X. Chen, *J. Am. Chem. Soc.*, 2011, **133**, 20661–20663.
11 H.-C. Liao, C.-C. Ho, C.-Y. Chang, M.-H. Jao, S. B. Darling and W.-F. Su, *Mater. Today*, 2013, **16**, 326–336.
12 S.-H. Liao, H.-J. Jhuo, Y.-S. Cheng and S.-A. Chen, *Adv. Mater.*, 2013, **25**, 4766–4771.
13 J. K. Lee, W. L. Ma, C. J. Brabec, J. Yuen, J. S. Moon, J. Y. Kim, K. Lee, G. C. Bazan and A. J. Heeger, *J. Am. Chem. Soc.*, 2008, **130**, 3619–3623.
14 T. Salim, L. H. Wong, B. Bräuer, R. Kukreja, Y. L. Foo, Z. Bao and Y. M. Lam, *J. Mater. Chem.*, 2011, **21**, 242–250.
15 C. Mc Dowell, M. Abdelsamie, M. F. Toney and G. C. Bazan, *Adv. Mater.*, 2018, E1707114.
16 M. Reichenberger, D. Kroh, G. M. M. Matrone, K. Schötz, S. Pröller, O. Filonik, M. E. Thordardottir, E. M. Herzig, H. Bässler, N. Stingelin and A. Köhler, *J. Polym. Sci., Part B: Polym. Phys.*, 2018, **56**, 532–542.
17 F. Zhao, C. Wang and X. Zhan, *Adv. Energy Mater.*, 2018, **8**, 1703147.
18 Z. He, Z. Zhang and S. Bi, *J. Mater. Sci.: Mater. Electron.*, 2019, **30**, 20899–20913.
19 U.-S. Jeng, C. H. Su, C.-J. Su, K.-F. Liao, W.-T. Chuang, Y.-H. Lai, J.-W. Chang, Y.-J. Chen, Y.-S. Huang, M.-T. Lee,

K.-L. Yu, J.-M. Lin, D.-G. Liu, C.-F. Chang, C.-Y. Liu, C.-H. Chang and K. S. Liang, *J. Appl. Crystallogr.*, 2010, **43**, 110–121.
20 D.-M. Smilgies, *J. Appl. Crystallogr.*, 2009, **42**, 1030–1034.
21 S. J. Plimpton, *J. Comp. Physiol.*, 1995, **117**, 1–19.
22 Website. LAMMPS package, http://lammps.sandia.gov, accessed Feb. 2019.
23 H. Sun, *Macromolecules*, 1995, **28**, 701–712.
24 L. A. Girifalco, *J. Phys. Chem.*, 1991, **95**, 5370–5371.
25 L. Monticelli, *J. Chem. Theory Comput.*, 2012, **8**, 1370–1378.
26 O. A. Guskova, S. R. Varanasi and J.-U. Sommer, *J. Chem. Phys.*, 2014, **141**, 144303.
27 S. R. Varanasi, O. A. Guskova, A. John and J.-U. Sommer, *J. Chem. Phys.*, 2015, **142**, 224308.
28 P. V. Komarov, D. V. Guseva and P. G. Khalatur, *Polymer*, 2018, **143**, 200–211.
29 V. Sadovnichy, A. Tikhonravov, V. Voevodin and V. Opanasenko*Contemporary High Performance Computing: From Petascale toward Exascale*, CRC Press, Boca Raton, USA, 2013, p. 283.

